Protein Structure and Folding:

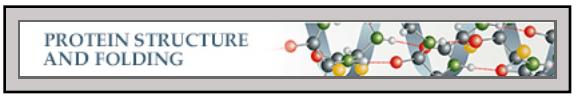

The α1.α2 Network of Collagen IV: REINFORCED STABILIZATION OF THE NONCOLLAGENOUS DOMAIN-1 BY NONCOVALENT FORCES AND THE ABSENCE OF MET-LYS CROSS-LINKS

Roberto M. Vanacore, Sivananthaperumal Shanmugasundararaj, David B. Friedman, Olga Bondar, Billy G. Hudson and Munirathinam Sundaramoorthy

J. Biol. Chem. 2004, 279:44723-44730.
doi: 10.1074/jbc.M406344200 originally published online August 5, 2004

THE JOURNAL OF BIOLOGICAL CHEMISTRY
Vol. 279, No. 43, Issue of October 22, pp. 44723–44730, 2004
Printed in U.S.A.

The α1.α2 Network of Collagen IV

REINFORCED STABILIZATION OF THE NONCOLLAGENOUS DOMAIN-1 BY NONCOVALENT FORCES AND THE ABSENCE OF MET-LYS CROSS-LINKS*

Received for publication, June 7, 2004, and in revised form, August 4, 2004
Published, JBC Papers in Press, August 5, 2004, DOI 10.1074/jbc.M406344200

Roberto M. Vanacore‡§, Sivananthaperumal Shanmugasundararaj¶‖, David B. Friedman§‡‡, Olga Bondar¶‖, Billy G. Hudson§¶‖, and Munirathinam Sundaramoorthy§¶‖§§**

*From the ‡Department of Biochemistry and Molecular Biology, Kansas University Medical Center, Kansas City, Kansas, 66160, the ¶Division of Nephrology, Department of Medicine, the ‖Center for Matrix Biology, the §Department of Biochemistry, and the **Mass Spectrometry Research Center, Vanderbilt University Medical Center, Nashville, Tennessee, 37232-2372*

Collagen IV networks are present in all metazoa and underlie epithelia as a component of basement membranes. The networks are essential for tissue function and are defective in disease. They are assembled by the oligomerization of triple-helical protomers that are linked end-to-end. At the C terminus, two protomers are linked head-to-head by interactions of their trimeric noncollagenous domains, forming a hexamer structure. This linkage in the α1.α2 network is stabilized by a putative covalent Met-Lys cross-link between the trimer-trimer interface (Than, M. E., Henrich, S., Huber, R., Ries, A., Mann, K., Kuhn, K., Timpl, R., Bourenkov, G. P., Bartunik, H. D., and Bode, W. (2002) *Proc. Natl. Acad. Sci. U. S. A.* 99, 6607–6612) forming a nonreducible dimer that connects the hexamer. In the present study, this cross-link was further investigated by: (*a*) comparing the 1.5-Å resolution crystal structures of the α1.α2 hexamers from bovine placenta and lens capsule basement membranes, (*b*) mass spectrometric analysis of monomer and nonreducible dimer subunits of placenta basement membrane hexamers, and (*c*) hexamer dissociation/re-association studies. The findings rule out the novel Met-Lys cross-link, as well as other covalent cross-links, but establish that the nonreducible dimer is an inherent structural feature of a subpopulation of hexamers. The dimers reflect the reinforced stabilization, by noncovalent forces, of the connection between two adjoining protomers of a network. The reinforcement extends to other types of collagen IV networks, and it underlies the cryptic nature of a B-cell epitope of the α3.α4.α5 hexamer, implicating the stabilization event in the etiology and pathogenesis of Goodpasture autoimmune disease.

Collagen IV is a major protein component of basement membranes, a specialized form of extracellular matrix underlying epithelia that compartmentalizes tissues and provides molecular signals for influencing cell behavior. The collagen IV family is composed of six α-chains (α1 to α6) that assemble into three kinds of triple-helical protomers (1). Each protomer has three functional domains, a 7S domain at the N terminus, a long triple-helical collagenous domain in the middle of the molecule, and a noncollagenous (NC1)[1] domain trimer at the C terminus. Protomers self-assemble into networks by end-to-end associations that connect four molecules at the N terminus, forming a 7S tetramer, and two molecules at the C terminus, forming a NC1 domain hexamer (1). Three types of networks are known: an α1.α2 network present in the basement membranes of all metazoa and an α3.α4.α5 network and an α1.α2-α5.α6 network that have restricted distributions. The networks are essential for tissue function, because they provide mechanical stability, provide a scaffold for assembly of other macromolecules, and serve as ligands for integrins (1–3).

The NC1 domain plays a pivotal role in the assembly of distinct networks. The specificity for chain selection is governed by recognition sequences encoded within NC1 domains of the respective six α-chains (4, 5). In protomer assembly, the NC1 domains (monomers) of three chains interact, forming an NC1 trimer, to select and register chains for triple-helix formation. In network assembly, the NC1 trimers of two protomers interact, forming an NC1 hexamer structure, to select and connect protomers. This trimer-trimer interface is stabilized by a putative covalent cross-link, which may exist in all three collagen IV networks (6).

The existence of cross-links (reducible and nonreducible) was first proposed from studies of the NC1 hexamer isolated by collagenase digestion of α1.α2 collagen IV networks of human placenta, aorta, and mouse tumor (7, 8). Upon exposure to acidic pH or denaturants, the NC1 hexamer dissociates into monomers and dimers, the later reflecting the cross-links. Subsequent studies of α1.α2, α3.α4.α5, and α1.α2-α5.α6 collagen IV networks have shown that the cross-links connect α1-like monomers (α1-α1, α1-α5, and α3-α5) and α2-like monomers (α2-α2, α2-α6, and α4-α4) (9, 10). For two decades, the reducible dimers were thought to be disulfide-linked monomers (7, 11). However, the recent x-ray crystal structures of the NC1 hexamers of bovine lens capsule basement membrane (LBM) and human placenta basement membrane (hPBM), determined

* This work was supported in part by Grants DK18381 (to B. G. H.), DK065123 (to B. G. H.), DK62524 (to M. S.), and RR017806 (to D. B. F) from the National Institutes of Health. The costs of publication of this article were defrayed in part by the payment of page charges. This article must therefore be hereby marked "*advertisement*" in accordance with 18 U.S.C. Section 1734 solely to indicate this fact.

The atomic coordinates and structure factors (codes 1T60 and 1T61) have been deposited in the Protein Data Bank, Research Collaboratory for Structural Bioinformatics, Rutgers University, New Brunswick, NJ (http://www.rcsb.org/).

‡‡ Received institutional support from Vanderbilt University through the Academic Venture Capital Fund.

§§ To whom correspondence should be addressed. Tel.: 615-322-8142; Fax: 615-322-7156; E-mail: m.sundaramoorthy@vanderbilt.edu.

[1] The abbreviations used are: NC1, noncollagenous domain; LBM, lens capsule basement membrane; PBM, placenta basement membrane; hPBM, human PBM; MALDI, matrix-assisted laser desorption and ionization; TOF, time-of-flight; MS, mass spectrometry; MS/MS, tandem mass spectrometry; MAD, multiwavelength anomalous dispersion; bicine, *N*,*N*-bis(2-hydroxyethyl)glycine; HPLC, high-performance liquid chromatography; r.m.s., root mean square.

independently by us (4) and Than *et al.* (6), respectively, have disproved this hypothesis. Both hexamers showed only intrachain disulfides with no possibility of forming interchain disulfides without destabilizing the two trimeric caps of the hexamer. For the nonreducible cross-link, a novel thioether cross-link was reported by Than *et al.* (6) involving a methionine (Met^{93}) residue and a lysine (Lys^{211}) in the hPBM hexamer; the evidence was based on electron density maps at 1.9 Å suggesting the existence of both cross-linked and uncross-linked residues at this site. The existence of this novel thioether cross-link is surprising given that the NC1 hexamer of *Hydra vulgaris* collagen IV dissociates into both monomers and dimers but is devoid of the equivalent Met and Lys residues (12, 13). Instead, it has glutamate residues at these positions.

In the present study, the chemical nature of the putative Met-Lys cross-link was further investigated. This was achieved by (*a*) increasing the diffraction resolution of crystals of hexamers of bovine placenta basement membrane (PBM) and of lens capsule basement membrane (LBM) to 1.5 Å and comparing their structures, (*b*) mass spectrometric analysis of monomer and nonreducible dimer subunits of PBM hexamers, and (*c*) hexamer dissociation and re-association studies. The findings rule out the novel Met-Lys cross-link, as well as other covalent cross-links, but reveal the existence of metal ions that may reinforce the stability of the trimer-trimer interface. Also, this study establishes that the nonreducible dimer is an inherent structural feature of a subpopulation of hexamers. The dimer reflects the reinforced stabilization, by noncovalent forces, of the connection between two adjoining protomers of a network. The reinforcement extends to other types of collagen IV networks, and it underlies the cryptic nature of a B-cell epitope of the $\alpha3.\alpha4.\alpha5$ hexamer, implicating the stabilization event in the etiology and pathogenesis of Goodpasture autoimmune disease (27).[2]

EXPERIMENTAL PROCEDURES

Crystallization and Data Collection—NC1 hexamers of bovine LBM and PBM were purified by collagenase digestion as previously described (14). Crystals of LBM hexamers were grown according to Sundaramoorthy *et al.* (4). The crystallization medium contained 10% polyethylene glycol 20,000, 0.1 M bicine, pH 9.0, and 5% 2-methyl-2,4-pentanediol. The crystals belong to the $P2_1$ space group with four hexamers in the asymmetric unit. The PBM hexamer crystals were grown using the hanging drop, vapor diffusion method at nearly identical conditions, except that 2-methyl-2,4-pentanediol was replaced by dioxane. However, the PBM protein crystallized differently in the $P2_12_12_1$ space group with one hexamer in the asymmetric unit. Complete datasets extending to 1.5 Å for both LBM and PBM hexamer crystals were collected at cryogenic temperature at Stanford Synchrotron Radiation Laboratory, beamline 9-1 (Mar365 imaging plate) and Advanced Photon Source, Southeast Regional Collaborative Access Team (SER-CAT) beamline (MarCCD), respectively, and processed using DENZO and SCALEPACK of the HKL2000 suite (15) (Table I).

Structure Determination and Refinement—The 2.0-Å resolution LBM hexamer coordinates (PDB accession code: 1M3D, chains A–F) were used as the search model in the molecular replacement calculations. The calculations were performed using the AmoRe (16) program of the CCP4 suite, which provided solution for one hexamer in the case of PBM crystal and four hexamers for LBM crystal. Initial models were subjected to rigid body refinement using 30.0–3.0 Å data followed by simulated annealing refinement using reflections in 10.0- to 2.5-Å resolution range. This and subsequent refinements were carried out using CNS (17) and cross-validated by the calculation of R_{free} using 5% of randomly selected reflections. After this stage, few rounds of positional and individual *B*-factor refinements were carried out while gradually increasing the resolution to 2.0 Å. From this point each round of positional and *B*-factor refinements were followed by the addition of solvent molecules using the standard criteria. Adjustments of models were made at the end of each refinement cycle guided by $2F_o - F_c$ and $F_o - F_c$ maps using O graphics software (18). These iterative processes were continued until the highest resolution of 1.5 Å was reached for both data sets, and all the model errors were satisfactorily corrected, including solvent modeling. In the final rounds of refinement, nonbonded energy restraints for the side chains of $Met^{93/90}$ and $Lys^{211/209}$ were removed. The refined models were analyzed using SETOR (19), PROCHECK (20), HBPLUS (21), and the Internet-based protein-protein interaction server (www.biochem.ucl.ac.uk/bsm/PP/server/).

Gel Electrophoresis and Chromatography—Crystals of both PBM and LBM hexamers were harvested separately in their artificial mother liquors. The crystals were washed thoroughly in fresh mother liquor to remove uncrystallized protein. Clean crystals were redissolved in buffer and used in electrophoresis and chromatography analyses. Polyacrylamide gels of 4–20% linear gradient (Bio-Rad) were used. PBM and LBM hexamers were boiled in sample buffer for 5 min before loading. Gels were stained with Coomassie Brilliant Blue R-250. For chromatography analyses, PBM and LBM hexamers were boiled for 10 min in 4 M guanidine-HCl, 0.05 M Tris-HCl, pH 7.5. Dimers and monomers were separated using a TSK-G3000sw ToSo-Hass HPLC column equilibrated with 4 M guanidine-HCl.

Dissociation and Re-assembly of NC1 Domain Hexamers—NC1 hexamers of LBM and PBM were dissociated in 50 mM formic acid buffered at pH 3.0 with Tris base (5). Under this condition the dissociation into monomers and dimers occurred, as verified by using TSK-G3000 ToSo-Hass HPLC gel filtration column. The dimer and monomer fractions were separated and used for re-assembly studies. The pure monomer (LBM) and dimer (PBM) fractions were re-associated separately by changing the buffer to TBS, pH 7.5. The sample was concentrated to about 1 mg/ml and incubated for 24 h at room temperature. The reassembled hexamers were analyzed by HPLC gel filtration and by SDS-PAGE.

Mass Spectrometry—PBM hexamers were denatured in 4 M guanidine-HCl and 50 mM dithiothreitol by boiling in a water bath for 20 min, and subsequently alkylated with 0.25 M iodoacetamide. Dimers and monomers were size-separated by HPLC in 4 M guanidine-HCl. Each fraction was digested with sequencing-grade trypsin (Promega) at 1:25 enzyme to protein ratio by incubating overnight at room temperature. Tryptic peptides were Zip-Tip (Millipore)-cleaned and combined with a α-cyanohydroxycinnamic acid matrix for matrix-assisted laser desorption/ionization, time-of-flight mass spectrometry (MALDI-TOF MS) analysis using a Voyager 4700 mass spectrometer (Applied Biosystems). The peptides were initially identified by comparing the experimental masses of each peak with computer-predicted masses of tryptic peptides from the bovine $\alpha1$ NC1 (IV) and $\alpha2$ NC1 (IV) sequences (4). The identity of some peptide sequences was confirmed by inducing ion fragmentation using the instrument in the tandem mode (MS/MS).

RESULTS AND DISCUSSION

Previously, the crystal structures of NC1 hexamers from LBM and hPBM were refined at 2.0 Å and 1.9 Å, respectively (4, 6). The two structures are virtually identical except for the amino acid differences between the bovine and human sequences. The only other difference that distinguishes the two structures is a set of partial Met-S^{δ}-Lys-C^{ϵ} thioether cross-links at the hexamer interface reported for hPBM structure (6), which, however, is completely absent in LBM structure (4). The partial cross-links were modeled in hPBM structure based on residual electron density peaks observed between the side chains of Met^{93} and Lys^{211} belonging to two opposing α-chains. In this context, we crystallized bovine PBM hexamer as well as LBM hexamer to obtain higher resolution diffraction data for more accurate refinement of the model, especially of the Met-Lys pairs at the hexamer interface. The crystals were also redissolved in the buffer and used in all other experiments. The use of crystallized protein in all experiments provides an unambiguous correlation of the results from x-ray crystallography, electrophoresis, and mass spectrometry.

Structure Refinement—PBM and LBM hexamers crystallized using nearly identical conditions pack in two different lattice forms. The former packs in an orthorhombic lattice ($P2_12_12_1$) with only one hexamer in the asymmetric unit and the latter in a monoclinic space group ($P2_1$) with four hexamers in the asymmetric unit. Both crystal forms diffracted to

[2] D.-B. Borza, O. Bondar, S. Colon, P. Todd, Y. Sado, and B. G. Hudson, manuscript in preparation.

TABLE I
Summary of crystallographic analysis

	PBM	LBM
Data collection		
Unit cell		
a (Å)	73.65	127.39
b (Å)	80.14	140.14
c (Å)	235.42	160.69
β (°)		91.26
Space group	$P2_12_12_1$	$P2_1$
No. molecules in ASU	1	4
Resolution (Å)	1.5	1.5
No. of observations	760,633	1,646,755
No. of reflections	215,169	859,512
Completeness (%)	96 (85)[a]	96.5 (97.8)
R_{sym} (%)	8.8 (26.4)	7.5 (68.0)
I/σ(I)	12.4 (1.2)	13.9 (1.0)
Refinement		
Resolution range (Å)	8.0–1.5	8.0–1.5
No. of reflections used ($\sigma > 2$)	163,779/8,188	608,966/31,862
Working/test		
R_{cryst}/R_{free} (%)	17.5/19.9	19.0/21.8
Average *B*-factor (Å)	15.49	21.73
No. protein atoms	10,365	41,681
No. of non-protein atoms	729	3118
r.m.s. deviation		
Bond lengths (Å)	0.0058	0.0072
Bond lengths (°)	1.35	1.38

[a] Values in the parentheses are for the highest resolution shells.

higher resolutions than previously reported, and datasets extending to 1.5 Å were collected from a single crystal for each protein. The structures were solved by molecular replacement method and were refined to R_{factor}/R_{free} of 0.175/0.199 and 0.190/0.218 for PBM and LBM crystals, respectively. Summaries of data collection and refinement statistics are provided in Table I. The final model of PBM crystal structure consists of 1 hexamer comprising chains A–F, 8 cations, 6 anions, and 708 solvent molecules and that of LBM crystal consists of 4 hexamers comprising chains A–X, 16 cations, 24 anions, and 3044 solvent molecules.

Description of Overall Structure—The backbone atoms of four hexamers of the LBM crystal asymmetric unit superimpose with an r.m.s. deviation of 0.73–0.76 Å. Similarly, the superimposition of PBM hexamer on different LBM hexamer backbones results in an r.m.s. deviation of 0.75–0.79 Å for the backbone atoms. These figures indicate that there are no significant differences in the overall structures within or between the two crystal forms. The two different crystal packings show no obvious structural differences in the crystal contact regions. Fig. 1 shows the *ribbon diagram* depicting the overall architecture of a typical NC1 hexamer (PBM). Overall, the NC1 hexamer forms a compact ellipsoid-shaped structure formed by two trimers related by a noncrystallographic 2-fold symmetry. The hexamer or trimer-trimer interface is formed by a large flat surface covering about 4000 Å^2 of solvent-accessible surface area. Each trimer is made up of two α1 chains and one α2 chain related by a pseudo 3-fold symmetry. The monomers within a trimer interact very tightly through three-dimensional domain swapping interactions to form a stable scaffold of six-strand antiparallel β-sheet with a two-strand β-hairpin of one chain inserting into the adjacent chain (4). Additionally, the three monomer-monomer interfaces contain unique sites of interaction that provide basis for chain-specific assembly of the trimer. The NC1 domain of each α-chain contains 12 cysteines, and all of them are involved in disulfide bonds. Each monomer is composed of two similarly folded subdomains, N- and C-domains, which contain three intradomain disulfides each at identical positions. Both LBM and PBM hexamer structures showed only intrachain disulfides. The high resolution crystal structures show disordered N- and C-terminal regions of both α1 and α2 chains. Similarly, post-translational modifications such as glycosylation were not detected in either of the structures.

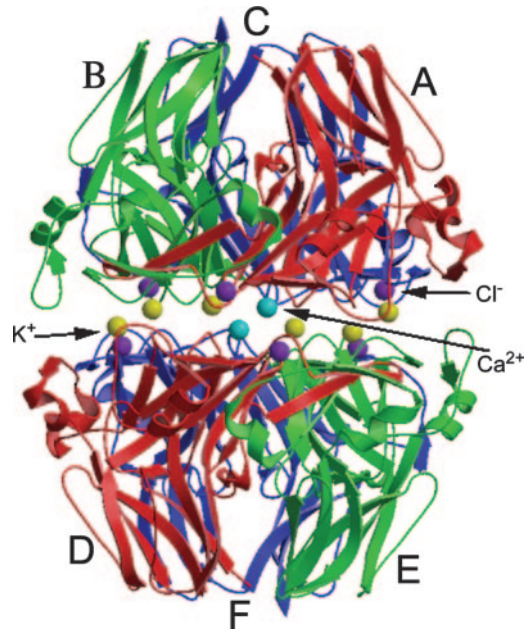

FIG. 1. **Ribbon model for the PBM hexamer at 1.5-Å resolution down the 2-fold NCS axis.** The chains of the NC1 hexamer are shown with different colors as follows: α1 (*A* and *D*, *red*; *B* and *E*, *green*) and α2 (*C* and *F*, *blue*). Chains A, B, and C make up the upper trimer, whereas chains D, E, and F compose the lower trimer. Potassium, calcium, and chloride ions are indicated with *spheres* colored in *yellow*, *cyan*, and *purple*, respectively. The figure was made with Bobscript (25) and rendered using Raster3D (26).

Analyses of NC1 Hexamer Interface: Search for Covalent Cross-links—Instead of disulfide cross-links, Than *et al.* (6) reported the occurrence of a novel thioether cross-link involving a methionine (Met^{93}) and a lysine (Lys^{211}) in the structure of the hPBM hexamer. These residues are contributed by two different chains of two interacting trimers and are located at the hexamer interface. They were modeled in two sets of conformations based on the electron density map at 1.9-Å resolution, one unlinked and the other covalently linked. There are two Met-Lys cross-links per pair of chains, and hence six such cross-links per hexamer are possible. The support for the cross-link stems from the observation of a weak positive peak between the two residues in the difference electron density map. They also claimed, without providing details, to have confirmed the cross-linked peptides from the size-separated tryptic peptides of dimers, but not from the monomers. However, superimposition of the 2.0-Å LBM hexamer structure (1M3D), in which cross-links were not detected, with hPBM hexamer structure (1LI1) shows remarkable resemblance, including the location of the putative cross-link-forming residues, Met^{93} and Lys^{211} (The coordinates for only uncross-linked conformations of these two residues are available in the Protein Data Bank).

Now that the refinement of two structures at 1.5 Å of the same protein (LBM and PBM) from two different tissues, lens capsule and placenta, of the same species are completed, we have superior models for objective comparison. Thus, simulated annealing omit maps were computed for each of Met-Lys pairs in both structures (Fig. 2). The maps do not show continuous density linking the two residues in any of the six possible sites in PBM structure as would be expected for covalent bonds. They appear generally disordered as commonly observed for solvent-exposed methionine and lysine residues in most crystal structures of proteins. However, some pairs show much clearer density for the side chains, and those pairs are clearly away

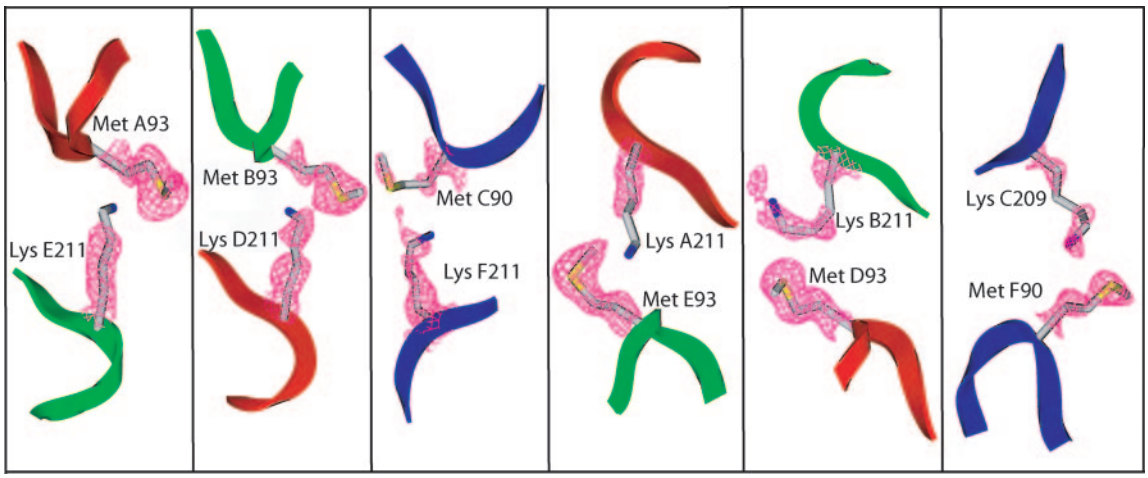

FIG. 2. **Electron density for the side chains of Met$^{93/90}$ (α1/α2) and Lys$^{211/209}$ (α1/α2) at the PBM hexamer interface.** The $F_o - F_c$ omit electron density map around Met$^{93/90}$ and Lys$^{211/209}$ is contoured at 2.5σ and colored *purple*. The figure was made with SETOR (19).

from each other, implying that they do not form covalent bonds (Fig. 2). Refinement of the structures without nonbonded energy restraints for the methionine and lysine residues involved in the putative cross-links did not move the side-chain atoms significantly. In some instances, the ϵ-amino group of Lys^{211} is within hydrogen bonding distance (~2.7 Å) from the carbonyl oxygen of Met^{91} of the opposite trimer. Although, the residues Met^{93} and Lys^{211} are indeed the closest pair at the interface as observed in the high resolution structures, there is no significant residual electron density between them to be interpreted as a potential covalent bond. The distance measured between Lys^{211}-C$^{\epsilon}$ and Met^{93}-S$^{\delta}$ ranged (for the six putative sites in the hexamer) between 2.5 and 3.5 Å, which is beyond the expected distance of 1.8 Å for a thioether bond (22). Thus, the 1.5-Å crystal structures of LBM and PBM hexamers rule out the proposed Met-Lys cross-link reported by Than *et al.* (6) and show no evidence for cross-links that could account for the dimer subunits observed upon hexamer dissociation.

Protein-Ion Interactions—The major difference between the LBM and PBM hexamer structures was observed during the modeling of solvent structure. The electron density map of PBM crystal showed strong peaks at specific sites in all the six chains. These sites, when modeled with water molecules, refined to the lowest *B*-factor limit (1 Å^2) set in the refinement and still showed strong residual density in difference Fourier map. Corresponding sites in LBM structure show significantly lower density. This indicated that these sites are occupied by electron dense ions in PBM structure rather than water molecules, and it is quite possible that the LBM structure has partially occupied ions or solvent molecules. The high electron density sites could be clearly divided into three groups based on their chemical environment and hence modeled with three kinds of ions. Because there was very little prior knowledge on the nature of the ions, we used certain chemical and crystallographic parameters as the criteria during the trial-and-error modeling of the sites.

The first group consists of six sites located at the hexamer interface. Each of them interacts with three α-chains, two from one trimer and the third from the opposing trimer (Fig. 3, *A* and *B*). The ligands are predominantly negatively charged and so are assumed to be coordinated by cations. After modeling several different cations, it was narrowed down to either K^+ or Ca^{2+} based on flattening of the difference density after the refinement. The *B*-factors of these cations were also refined to values comparable to those of their ligands. Because the Ca^{2+} ion is invariably coordinated to oxygen ligands and its coordination distances are shorter than the ones observed, it was concluded that these sites are most likely occupied by K^+ ions (Table II).

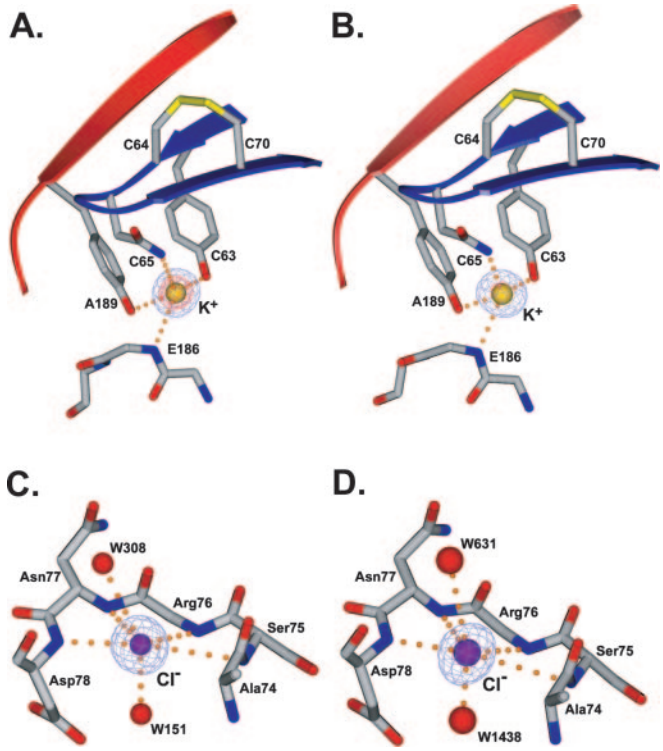

FIG. 3. **Metal binding sites of NC1 hexamers: specific metal-protein interactions.** *A* and *B* display the side-chain ligands around one of the six potassium ions found in PBM and LBM hexamers, respectively. The spherical electron-density peak observed in the difference Fourier omit map is contoured at 2.5 σ (*purple*) and 15 σ (*red*). The K^+ ion is shown as a *space-filling model* colored in *gold*. Chain coloring is as in Fig. 2. *C* and *D* represent one of the chloride binding sites found in PBM and LBM hexamers, respectively. The *spherical* electron-density peak of the $F_o - F_c$ omit map is contoured at 2.5 σ, and the Cl^- ion is shown as a *space-filling model* colored in *purple*. The figure was made with SETOR (19).

The example shown in Fig. 3 contains hydroxyl groups of Tyr^{189} and Tyr^{63}, one each from chains α1A and α2C, and an amino group of Asn^{65} from chain α2C from one trimer and a backbone amide nitrogen (Arg^{186}) of chain α1E from the other trimer. Sequence differences between α1 and α2 NC1 domains originate two homologous but slightly different ion coordination environments. Whereas the β-hairpin from the α2 chain provides two ligands for metal binding, the equivalent segment

TABLE II
Potassium binding sites: coordination distances and refinement parameters

Chains	Ligands	Distance		Occupancy[a]		*B*-factor[b]	
		PBM	LBM	PBM	LBM	PBM	LBM
		Å		%		Å²	
α2.α1.α1	Tyr^{63} (OH)	3.06	3.06	88	66	11.23	19.37
	Asn^{65} (Nδ2)	3.38	3.34				
	Ala^{186} (amide)	3.20	3.35				
	Tyr^{189} (OH)	3.05	2.83				
α1.α2.α2	H_2O	3.28	3.14	89	86	11.87	15.53
	Asn^{66} (Nδ2)	3.26	3.23				
	Ala^{84} (amide)	3.17	3.16				
	Tyr^{187} (OH)	3.17	3.12				
α1.α1.α1	H_2O	3.32	3.25	84	0[c]	15.18	
	Asn^{66} (Nδ2)	3.49	5.51				
	Ala^{186} (amide)	3.20	3.09				
	Tyr^{189} (OH)	3.18	2.94				

[a] Refined occupancy with potassium *B*-factor set to the average of *B*-factors of the ligands.
[b] Refined *B*-factor with potassium occupancy set at 1.0.
[c] These sites were modeled as water molecules.

of α1 provides coordination by Asn^{66} only because Phe^{64} replaces the second ligand tyrosine. In this case, a water molecule substitutes the missing hydroxyl group. Certainly, the fact that these coordination sites are located at the hexamer interface suggests that the metal ions may reinforce both intra-protomer as well as inter-protomer interactions. Based on the number of coordinating ligands, the trimer structure would benefit further from the metal-protein interactions by reinforcing of the six-stranded β-sheet formed by adjacent α-chains. However, the additional metal-protein interactions across the hexamer interface may also contribute to the remarkable stability of the hexamer.

In the LBM hexamer, two out of the six potassium sites were modeled as solvent molecules (Table II), because their peak heights were significantly and consistently lower among all four hexamers in the asymmetric unit. The refinement of these two sites with water molecules flattened the difference map, and their thermal parameters matched with those of the surrounding ligands. Furthermore, the side chain of Asn^{65} in the α2 chain swings away from the coordination site, suggesting that the site is not occupied by an ion requiring amino acid ligands but occupied by a solvent molecule with a minimum number of hydrogen bonding interactions (Table II).

The potassium sites were uniformly occupied by Br^- ions at all six locations in 2.0-Å LBM hexamer structure (4) and similarly, acetate ions were found in the 1.9-Å hPBM hexamer structure (6). The conformations of the coordinating amino acid ligands were similar in all the sites in each structure. The LBM hexamer crystal was soaked in 0.5 M potassium bromide for MAD phasing, and hPBM crystals were grown in 3 M sodium acetate. However, the crystals of LBM and PBM hexamer in the present study were grown under similar conditions using proteins purified by similar protocols and in the absence of high concentration of salt. However, the putative ion binding sites in the two structures show completely different pictures. Whereas all sites in the PBM structure are uniformly occupied by a strong peak with all the available ligands in coordinating conformations, the sites in LBM structure are heterogeneous with different extent of electron density peaks and variability in the conformation of the asparagine ligand. Thus, it is clear that the protein has a potential set of ligands for coordination when a suitable ion is available. Because potassium salts were not added exogenously in high concentration during purification or crystallization, the ions found in 1.5-Å structure of the PBM hexamer must have an endogenous origin. In addition, the coordinating ligands are conserved among the mammalian α-chains, suggesting that this structural feature is conserved. Therefore, it is tempting to speculate that occupation of these metal binding sites might act as a regulatory factor in regard to hexamer stability.

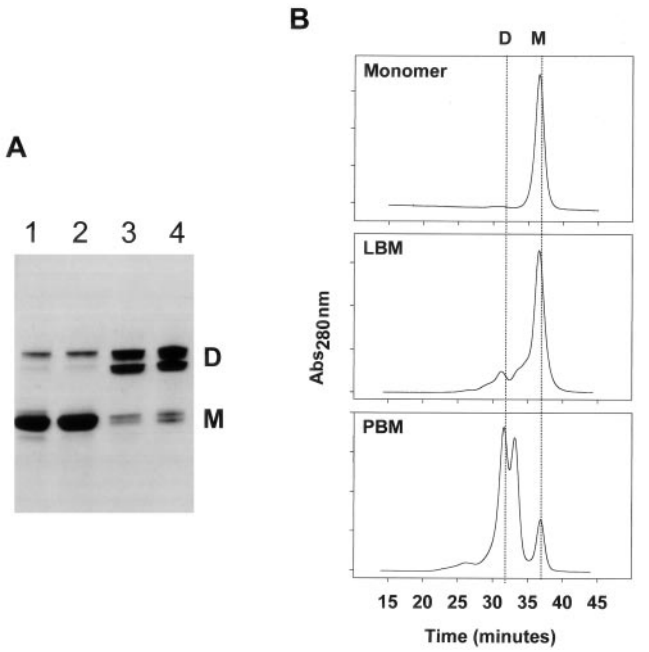

FIG. 4. **Analyses of the dissociative properties of the crystallized form of LBM and PBM hexamers.** *A*, electrophoretic profile of LBM hexamer before (*1*) and after (*2*) crystallization and PBM hexamer before (*3*) and after (*4*) crystallization. *D* and *M* indicate the position of dimers and monomers, respectively. *B*, chromatographic profile of NC1 hexamers in denaturing conditions. The column, equilibrated in guanidine-HCl, separated monomers (*M*) from dimers (*D*). The *upper panel* is the control recombinant α2NC1 monomer. The *middle panel* is the LBM hexamer, and the *lower panel* is the PBM hexamer.

The second group of ions consists of six identical sites in each of the six chains. They are located in the loop comprising amino acids Ala^{74}-Asp^{78} (Fig. 3, *C* and *D*). Each of the sites is linked to three backbone amide groups and two potential water peaks. These were the locations of strong Br^- binding sites in the structures of both LBM and hPBM, which were determined using a Br-MAD phasing method by soaking their crystals in high concentrations of KBr/NaBr. The positive amide ligands and the knowledge from the halide-MAD experiments prompted us to conclude that these sites must be anionic. Therefore, they were modeled as Cl^- sites, because NaCl was used in the buffers during purification. The *B*-factors of the Cl^- ions after the refinement were in the same range as those of their amide nitrogen ligands.

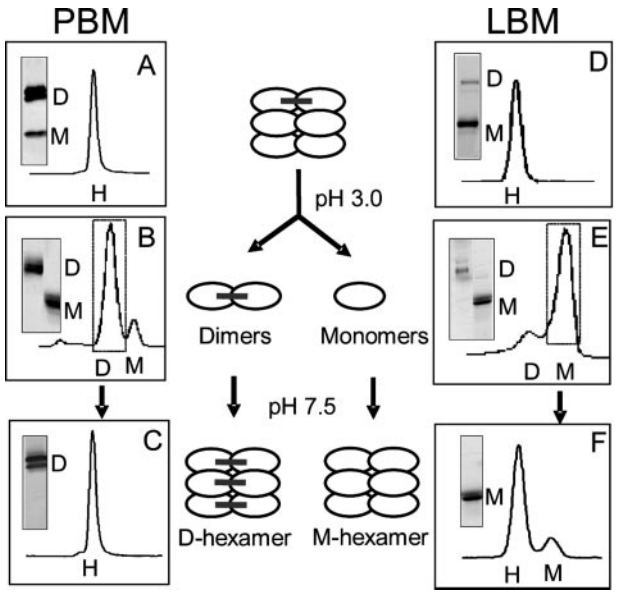

FIG. 5. **Dissociation of PBM and LBM hexamers and the re-association of monomer and dimer subunits into hexamers.** The *central panel* is a schematic of the dissociation/re-association experimental strategy. *A* and *B* show the elution time of a gel filtration HPLC column of the native hexamers of PBM and LBM, respectively. The *insets* in each panel show the monomer/dimer ratio analyzed by SDS-PAGE. Hexamer dissociation was induced with formic acid-Tris buffer pH 3.0. The profile of dissociated hexamers was examined by gel filtration HPLC, and the separation of the subunits was confirmed by SDS-PAGE (*B* and *E*). The purified dimer fraction of PBM was re-associated by exchanging buffer to Tris-buffered saline, pH 7.5, and incubated for overnight at room temperature. HPLC analyses of the re-associated dimer fraction from PBM shows a peak corresponding to hexamer elution time. This re-assembled hexamer composed of only dimer subunits is designated as D-hexamer (*C*). *Panel F* shows the same analyses for re-association of purified monomers fraction of LBM. A hexamer peak is also observed, which is designated M-hexamer. The *letters*, marking positions on the gels and HPLC profiles, designate *M* (monomer), *D* (dimer), and *H* (hexamer).

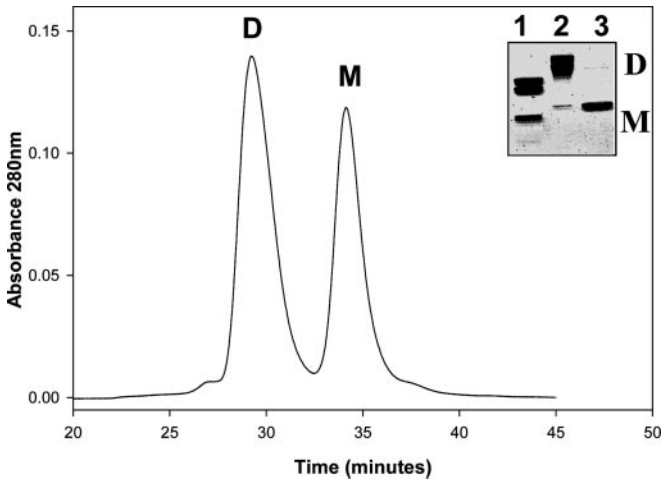

FIG. 6. **Isolation of monomer and nonreducible-dimer subunits from PBM hexamer by size-exclusion chromatography.** PBM hexamer dissociation was induced by reduction and alkylated in the presence of 4 M guanidine. Dimer (*D*) and monomer (*M*) fractions were separated on a TSK SW_{xl}3000 HPLC column equilibrated in 4 M guanidine. Each fraction was collected and analyzed on a SDS-PAGE (see *inset*).

In the PBM hexamer there are two more sites with large electron density, which were modeled as Ca^{2+} ions. Each Ca^{2+} ion is coordinated to the carboxylate groups of Asn^{148} and Glu^{149} belonging to the same α2 chain. The corresponding side chains in α1 chain are Ala^{149} and Gly^{150} with no possibility to bind a metal ion. Even though these ions are at the hexamer interface, they are unlikely to have any role in stabilizing the hexamer, because they are exclusively bound to a single α2 chain. The peaks at these sites in LBM hexamers are weak and were modeled as waters.

The Absence of Cross-linked Dimers Is Not an Artifact of Hexamer Crystallization or Dissociation—Because cross-linked dimers, as originally defined by SDS-PAGE (8), were not observed in the 1.5-Å crystal structure of the NC1 hexamers, it is possible that: (*a*) two distinct populations coexist, an M-hexamer composed exclusively of monomer subunits and a D-hexamer composed exclusively of cross-linked-dimer subunits and (*b*) the crystals were devoid of the cross-linked D-hexamer. To address this issue, we compared the subunit compositions of LBM and PBM hexamers before and after crystallization (Fig. 4). The relative proportions of dimers and monomers were identical for both crystallized and stock proteins for either LBM or PBM hexamers. Electrophoresis analysis of the residual crystallization drops, after the crystals were harvested, did not show any band, indicating that the protein was entirely incorporated into the crystals. Therefore, preferential crystallization of M-hexamer population does not explain the absence of cross-linked-dimers as indeed the crystals contained D-hexamers.

Alternatively, the absence of cross-linked dimers in the hexamer structure could be due to the fact that they are not an inherent structural feature of hexamers but an artifact of hexamer dissociation. This issue was addressed in two ways. First, the same samples that were used in the crystallization studies were dissociated under two conditions (4 M guanidine HCl and pH 3.0), and their subunits were analyzed by HPLC for comparison to the results of SDS-PAGE. The dimer/monomer ratio of 20:80 in LBM was identical for all three conditions of dissociation: SDS (Fig. 4*A*), guanidine (Fig. 4*B*), and low pH (Fig. 5), as was the 80:20 ratio for PBM, indicating that the dissociation patterns are independent of the type of protein-denaturing condition. These results confirm previous results (5, 9, 23), but, importantly, they directly establish the subunit compositions of the samples that were used in the crystallographic studies, allowing a correlation between the crystal studies (see above) and the distribution of subunits in hexamers (see below).

Second, the issue of an artifact was addressed by studying the dissociation/re-association of hexamers. Acid pH was chosen because it is the mildest among the three denaturant conditions and easier to reverse. At pH 3.0, LBM and PBM hexamers disassemble into dimer and monomer subunits, as determined by HPLC size-exclusion chromatography, which resolves these subunits (Fig. 5, *B* and *E*). Upon raising the pH to 7.5, the dimer fraction re-assembles into a hexamer, composed exclusively of dimers (Fig. 5*C*) and designated herein as D-hexamers. Upon incubation with SDS, the D-hexamer dissociates into cross-linked dimers but devoid of any monomer subunits (Fig. 5*C*, *inset*). In contrast, the monomer fraction re-assembles into a hexamer, composed exclusively of monomers (Fig. 5*F*) and designated as M-hexamers. Upon incubation with SDS, the M-hexamer dissociates into monomers but devoid of any dimer subunits (Fig. 5*F*, *inset*); had the cross-linked dimer been an artifact, the M-hexamer would have generated dimers. Collectively, these results indicate that dimers are an inherent structural feature of native hexamers not an artifact of hexamer dissociation. These findings, together with the absence of covalent cross-links in the crystals of hexamers, indicate that the dimers are held together by non-covalent interactions and not by Met-Lys cross-links.

Search for Met-Lys Cross-links by the Comparative Analyses of Monomers and Nonreducible Dimers by Mass Spectrometry—As an independent approach to x-ray crystallography, the

TABLE III
Tryptic peptides derived from bovine NC1 domains of Collagen IV

Chain	#	Sequence assignment	Predicted	Dimer observed	Monomer observed
			m/z	*m/z*	*m/z*
α1 NC1	T1	Ala^{212}-Arg^{216}	545.30	545.30	545.30
	T2[a]	Lys^{204}-Arg^{216}	1397.81	1397.81	1397.80
	T3[a]	Asn^{77}-Arg^{102}	3000.36	ND[b]	ND
	T4	Asn^{77}-Arg^{107}	3600.70	3600.69	3600.62
	T5[a]	T2 + T3	~4397	ND	
α2 NC1	T6	Ala^{210}-Arg^{214}	529.35	529.34	529.34
	T7	Tyr^{187}-Lys^{209}	2617.28	2617.30	2617.30
	T8[c]	Ser^{79}-Arg^{104}	3023.50	3023.48	3023.46
	T9[c]	Tyr^{187}-Arg^{214}	3127.61	3127.30	3127.30
	T10[c]	T7 + T8	~6151	ND	

[a] Tryptic peptides equivalent to the ones found as cross-linked peptides in Ref. 6.
[b] ND, not determined.
[c] This peptide sequence is followed by Pro^{103}, which makes the cleavage site resistant.

existence of the putative Met-Lys cross-links was further investigated by comparative analyses of monomers and nonreducible dimers using MALDI-TOF and tandem mass spectrometry (MS/MS). PBM hexamers were reduced and alkylated in 4 M guanidine-HCl to remove the fraction of dimer subunits that are sensitive to reduction. Nonreducible dimers and reduced monomers were separated on an HPLC column where each resolved as a single peak and distributed in a 60:40 ratio, respectively (Fig. 6). The separation of monomer and nonreducible dimer fractions was further analyzed by SDS-PAGE as shown in the *inset* of Fig. 6, *lines 2* and *3*, respectively. Each fraction was independently digested "in solution" with trypsin, and the peptide mixtures were analyzed by MALDI-TOF MS. We then performed a comparative analysis of the MALDI-TOF MS spectra of tryptic digest of monomers and nonreducible dimers to detect the putative Met-Lys cross-link as well as any other covalent cross-links. The mass spectral data of dimers and monomers showed very similar profiles suggesting chemical equivalency of the two fractions. Ions present in each spectrum were assigned with a tryptic peptide sequence derived from either α1 or α2 NC1 domain, leading to sequence coverage of each fraction of ~80% for both chains.

As shown in Table III, we determined the theoretical masses of tryptic peptides for the bovine NC1 domains, including or neighboring $Met^{93/90}$ and $Lys^{211/209}$ involved in the putative thioether cross-links. By adding the mass of the corresponding peptides, an estimate of the total mass of the cross-linked peptides was obtained. This mass range was examined extensively in each spectrum, both linear and reflectron mode, where known standards were observed (*e.g.* insulin *m/z* = 5730.6, data not shown). Surprisingly, the spectra showed no evidence for the Met-Lys cross-linked peptides (*m/z* = 4397 and *m/z* = 6151, Table III), despite accounting for ~80% sequence coverage. In contrast, the mass spectrum of both monomers and nonreducible dimers revealed the presence of uncross-linked tryptic peptides, including or neighboring the putative cross-linking residues. Fig. 7 represents a section of the mass spectrum of monomers and nonreducible dimers demonstrating the presence of a tryptic peptide containing the amino acid residue Met^{93}. As shown in Table III, tryptic peptides from every putative cross-linking site were found as uncross-linked peptides. Tandem MS (MALDI-TOF MS/MS) analysis of each peptide was consistent with the sequence assignment, which is confirmative of the identity of the peptides (Fig. 7*B*). It is noteworthy that the monomer and nonreducible dimer spectra revealed the presence of peptides T1, T6, and T7 (Table III), which is explained only by cleavage at Lys^{211} and Lys^{209} of the α1 and α2 NC1 domains, demonstrating that these sites are susceptible to trypsin, and, thus, they do not participate in a cross-link. Therefore, our results argue against the findings of Than *et al.* (6) by sequencing of tryptic peptides derived from

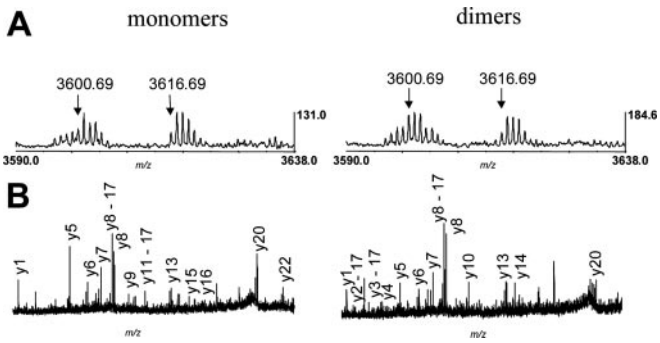

FIG. 7. **MALDI-TOF MS analysis of tryptic peptides from monomer and nonreducible dimer subunits of PBM hexamers.** The HPLC-separated dimer and monomer fractions (Fig. 6) were digested with trypsin and analyzed by MALDI-TOF MS as described under "Experimental Procedures." *A*, a segment of the mass spectrum demonstrating the detection of the Met^{93}-containing tryptic peptide (Table III, T4) from α1 NC1 sequence derived from the dimer and monomer fractions. *B*, fragmentation pattern and sequence assignment of peptide T4.

dimer in which cleavage at this site was not detected and hence, was interpreted as an evidence for the Met-Lys cross-link. In the present study, the mass spectrometry results were consistently reproducible in multiple experiments using several sample preparations of monomers and nonreducible dimers. Collectively, the mass spectrometry analyses rule out the Met-Lys cross-links.

Two Distinct Hexamer Populations: M-hexamers and D-hexamers—The dissociation/re-association studies (see above) establish that M- and D-hexamers can assemble *in vitro*, raising the question of whether they represent an inherent structural feature of native collagen IV networks. This issue was addressed by comparing the subunit compositions of native LBM and PBM hexamers. LBM hexamers are composed of 80% monomers and 20% dimers, whereas PBM hexamers are composed of 80% dimers and 20% monomers. These values are based on SDS-PAGE (*lanes 1* and *3*, Fig. 4*A*) and HPLC analyses under denaturing conditions of 4 M guanidine-HCl (Fig. 4*B*). In the case of LBM, the monomer/dimer ratio of 80:20 reflects the existence of at least two kinds of hexamers: 1) a population that is composed exclusively of monomers, designated as $M^{\alpha1.\alpha2}$-hexamers and that accounts for at least 40% and up to 80% of the hexamers and 2) one or more populations composed exclusively of dimers and/or a mixture of dimers and monomers and that accounts for at least 20% and up to 60% of the hexamers. In the case of PBM, the monomer/dimer ratio of 20:80 also reflects the existence of at least two kinds of hexamers: 1) a population that is composed exclusively of dimers, designated $D^{\alpha1.\alpha2}$-hexamers and that accounts for at least 40% and up to 80% of the hexamers and 2) one or more populations

composed exclusively of monomers ($M^{\alpha1.\alpha2}$-hexamers) and/or a mixture of monomers and dimers (M,D-hexamers), which accounts for at least 20% and up to 60%. Together, the subunit compositions of LBM and PBM hexamers provide unambiguous evidence for the existence of two distinct kinds of hexamers in native $\alpha1.\alpha2$-collagen IV networks: $M^{\alpha1.\alpha2}$-hexamers, composed exclusively of monomers, and $D^{\alpha1.\alpha2}$-hexamers, composed exclusively of dimers.

Concluding Remarks—The concept of covalent cross-links stabilizing NC1 hexamers is based on the observation that hexamers are composed of monomer and dimer subunits (7). Based on the effect of reduction on the behavior of dimers in SDS-PAGE, two kinds of covalent cross-links were envisaged to connect monomers forming a dimer, a disulfide-reducible cross-link, and a nonreducible cross-link. However, two recent reports on the x-ray structures of LBM and hPBM hexamers disproved the hypothesis of disulfide cross-linked dimers. In the hPBM study (6), the nonreducible cross-link was proposed to be a novel thioether linkage between Met and Lys.

In the present study, the nonreducible covalent cross-links were also ruled out, including the novel Met-Lys cross-link. The evidence is based on the high resolution 1.5-Å crystal structures of LBM and PBM hexamers, coupled with extensive mass spectrometric analyses of the nonreducible dimers. Instead, the NC1 hexamers are stabilized by noncovalent forces. Thus, we conclude that the nonreducible dimer subunits are held together by noncovalent forces rather than covalent cross-links.

The dimer subunits are an inherent structural feature of hexamers, not an artifact of hexamer dissociation as shown by the re-association studies. They are of two identities, an $\alpha1$NC1 homodimer and an $\alpha2$NC1 homodimer, as determined in earlier studies (7, 24). Based on the quaternary structure of an $\alpha1.\alpha2$ hexamer, the $\alpha1$ homodimers can be formed between monomers from either the same protomer or interacting protomers. However, the presence of only one $\alpha2$ monomer per protomer unambiguously establishes that the dimers are formed between monomers of the two protomers rather than within a protomer. Thus, the strong noncovalent forces holding the dimers together reinforce the stability of the protomer-protomer interface, thereby increasing the stability of the collagen IV network.

Furthermore, the search for cross-links by x-ray crystallography of LBM and PBM hexamers has brought forth an old observation that their dimer/monomer ratios are distinctly different. LBM hexamers, are composed mainly of monomers, whereas in PBM, predominantly of dimers (23). Based on the findings of the present study, this distinction can now be interpreted to reflect the existence of two kinds of hexamers, $M^{\alpha1.\alpha2}$-hexamers in LBM composed exclusively of monomers, and $D^{\alpha1.\alpha2}$-hexamers in PBM composed exclusively of dimers. The two extremes in subunit compositions reflect the existence of a process that reinforces the interaction of monomer subunits forming D-hexamers. The proportions of M- and reinforced D-hexamers indicate that the collagen IV network of PBM is a more stable structure than that of LBM, a feature that may be an important determinant of its biological function.

The exact nature of the noncovalent forces responsible for dimer assembly remains obscure. Possibly, the metal ions at the hexamer interface or unidentified post-translational modifications contribute to the assembly mechanism. The noncovalent forces may not be confined to a pair of residues locally, but rather encompass the entire interface between two monomers. These noncovalent forces are not unique to $\alpha1.\alpha2$ (IV) collagen network, but occur in the $\alpha3.\alpha4.\alpha5$ (IV) network as well.[2] In the latter case, the $D^{\alpha3.\alpha4.\alpha5}$-hexamers sequester B-cell epitopes from binding of autoantibodies, suggesting that reinforced stabilization of hexamers may be a crucial event in the etiology and pathogenesis of Goodpasture autoimmune disease.

Acknowledgments—We thank the Vanderbilt University's Center for Structural Biology for providing access to Biomolecular X-ray Crystallography Facility and SER-CAT beamline at the Advanced Photon Source. Use of the Advanced Photon Source was supported by the U. S. Department of Energy, Office of Science, Office of Basic Energy Sciences, under Contract No. W-31-109-Eng-38. Portions of this research were carried out at the Stanford Synchrotron Radiation Laboratory, a national user facility operated by Stanford University on behalf of the U. S. Department of Energy, Office of Basic Energy Sciences. The SSRL Structural Molecular Biology Program is supported by the National Institutes of Health, National Center for Research Resources, Biomedical Technology Program, and the National Institute of General Medical Sciences.

REFERENCES

1. Hudson, B. G., Tryggvason, K., Sundaramoorthy, M., and Neilson, E. G. (2003) *N. Engl. J. Med.* **348,** 2543–2556
2. Pöschl, E., Schlötzer-Schrehardt, U., Brachvogel, B., Saito, K., Ninomiya, Y, and U, M. (2004) *Development* **131,** 1619–1628
3. Guo, X., Johnson, J. J., and Kramer, J. M. (1991) *Nature* **349,** 707–709
4. Sundaramoorthy, M., Meiyappan, M., Todd, P., and Hudson, B. G. (2002) *J. Biol. Chem.* **277,** 31142–31153
5. Boutaud, A., Borza, D.-B., Bondar, O., Gunwar, S., Netzer, K.-O., Singh, N., Ninomiya, Y., Sado, Y., Noelken, M. E., and Hudson, B. G. (2000) *J. Biol. Chem.* **275,** 30716–30724
6. Than, M. E., Henrich, S., Huber, R., Ries, A., Mann, K., Kuhn, K., Timpl, R., Bourenkov, G. P., Bartunik, H. D., and Bode, W. (2002) *Proc. Natl. Acad. Sci. U. S. A.* **99,** 6607–6612
7. Siebold, B., Deutzmann, R., and Kuhn, K. (1988) *Eur. J. Biochem.* **176,** 617–624
8. Weber, S., Engel, J., Wiedemann, H., Glanville, R., and Timpl, R. (1984) *Eur. J. Biochem.* **139,** 401–410
9. Borza, D. B., Bondar, O., Ninomiya, Y., Sado, Y., Naito, I., Todd, P., and Hudson, B. G. (2001) *J. Biol. Chem.* **276,** 28532–28540
10. Borza, D.-B., Bondar, O., Todd, P., Sundaramoorthy, M., Sado, Y., Ninomiya, Y., and Hudson, B. G. (2002) *J. Biol. Chem.* **277,** 40075–40083
11. Weber, S., Dolz, R., Timpl, R., Fessler, J. H., and Engel, J. (1988) *Eur. J. Biochem.* **175,** 229–236
12. Sarras, M. P., Jr., Madden, M. E., Zhang, X. M., Gunwar, S., Huff, J. K., and Hudson, B. G. (1991) *Dev. Biol.* **148,** 481–494
13. Fowler, S. J., Jose, S., Zhang, X., Deutzmann, R., Sarras, M. P., Jr., and Boot-Handford, R. P. (2000) *J. Biol. Chem.* **275,** 39589–39599
14. Gunwar, S., Noelken, M. E., and Hudson, B. G. (1991) *J. Biol. Chem.* **266,** 14088–14094
15. Otwinowski, Z., and Minor, W. (1997) *Methods Enzymol.* **276,** 307–326
16. Navaza, J., and Saludjian, P. (1997) *Methods Enzymol.* **276,** 581–594
17. Brunger, A. T., Adams, P. D., Clore, G. M., DeLano, W. L., Gros, P., Grosse-Kunstleve, R. W., Jiang, J. S., Kuszewski, J., Pannu, N. S., Read, R. J., Rice, L. M., Simonson, T., and Warren, G. L. (1998) *Acta Crystallogr. Sect. D Biol. Crystallogr.* **54,** 905–921
18. Jones, T. A., and Kjeldgaard, M. (1997) *Methods Enzymol.* **277,** 173–208
19. Evans, S. V. (1993) *J. Mol. Graphics* **11,** 134–138
20. Laskowski, R. A., MacArthur, M. W., Moss, D. S., and Thornton, J. M. (1993) *J. Appl. Crystallogr.* **26,** 283–291
21. McDonald, I. K., and Thornton, J. M. (1994) *J. Mol. Biol.* **238,** 777–793
22. Ito, N., Phillips, S. E., Stevens, C., Ogel, Z. B., McPherson, M. J., Keen, J. N., Yadav, K. D., and Knowles, P. F. (1991) *Nature* **350,** 87–90
23. Langeveld, J. P., Wieslander, J., Timoneda, J., McKinney, P., Butkowski, R. J., Wisdom, B. J., Jr., and Hudson, B. G. (1988) *J. Biol. Chem.* **263,** 10481–10488
24. Gunwar, S., Ballester, F., Kalluri, R., Timoneda, J., Chonko, A. M., Edwards, S. J., Noelken, M. E., and Hudson, B. G. (1991) *J. Biol. Chem.* **266,** 15318–15324
25. Esnouf, R. (1999) *Acta Crystallogr. Sect. D Biol. Crystallogr.* **55,** 938–940
26. Merritt, E. A., and Bacon, D. J. (1997) *Methods Enzymol.* **277,** 505–524
27. Borza, B., Bondar, O., Todd, P. and Hudson, B. G. (2003) *J. Am. Soc. Nephrol.* **14,** 632A (Abstr. SU-PO451)